Wideband MIMO Channel Capacity Analysis based on Indoor Channel Measurement

Junjun Gao, Jianhua Zhang and Xiaofeng Tao
Key Laboratory of Universal Wireless Communications, Ministry of Education,
Beijing University of Posts and Telecommunications (BUPT), China
Email: {gaojunjun, jhzhang, taoxf}@bupt.edu.cn

***Abstract*—Based on the channel measurement in a typical indoor environment, wideband multi-input multi-output (MIMO) channel capacity analysis result is reported in this paper. A series of non line-of-sight (NLOS) and LOS measurement positions are planned for capacity comparison in different propagation conditions. For fixed received signal-to-noise ratio (SNR), slight average capacity loss in LOS cases is observed compared to N-LOS cases. However, the capacity in presence of LOS component appears more position-sensitive than that in NLOS cases. When considering the large scale path loss difference introduced by the receiver movement, the capacity in LOS cases greatly exceeds the NLOS cases. A key finding is that the measured maximum channel eigenvalue fits t Location-Scale distribution rather than Gamma distribution in indoor scenario. Finally, Ricean K-factor and spatial correlation results are presented.**

I. Introduction

Multi-input multi-output (MIMO) systems have attracted abundant research as its promising spectrum efficiency to meet the rapid data traffic growth requirement in indoor scenarios [1]. Unlike the outdoor environment, rich reflected and scattered components may be created by the regular building structure and surrounding indoor objects [2]. Despite of a high probability of LOS propagation in indoor environment, plenty multipaths bring additional degree of freedom due to the spatial diversity and frequency selective which provide favorable conditions for MIMO technique applications.

Channel measurement is the most straightforward and reliable method to acquire the real indoor channel characteristics and assess the channel capacity, which is important for future MIMO system deployment in indoor environment. There exists several literatures focusing on the indoor channel measurement from different perspectives. Effects of pedestrian movement on MIMO channel capacity have been experimentally investigated within indoor environment at 5.2 GHz [3]. Capacity and spatial correlation results including LOS and NLOS propagations inside a modern office are particularly discussed in [4]. Compared to NLOS scenarios, the results show that the capacity significantly decreases in LOS cases. On the other hand, it is observed that the angle of departure and arrival of the specular and dense multipath components (MPC) greatly varies as the change of the transmit (Tx) and receive (Rx) array positions [5]. The theoretical derivation of channel correlation given in [6] confirmed the coherent relationship between the spatial correlation and angle statistic information, which have great influence on the channel capacity. Hence, it can be deduced that the capacity in indoor environment is probably position-sensitive. However, only a few measurement positions were arranged in most of the previous indoor measurement literatures, which can not provide sufficient insight into indoor MIMO channel capacity especially the difference betweent the LOS and NLOS scenarios. Besides that, the path loss influence is usually ignored for capacity evaluation. As indicated in [7] that large scale fading plays an important role in capacity assessment, it should be taken into account for a reasonable fair performance evaluation. The maximum channel eigenvalue is a key parameter for the outage probability and symbol error rate (SER) analysis of MIMO beamforming systems [8]. The measured maximum eigenvalue p.d.f. is experimently proved to fit the Gamma distribution in outdoor NLOS environment [9]. However, the eigenvalue statistics in indoor LOS and NLOS cases have not been well studied yet.

A set of LOS and NLOS measurement positions have been planned in a typical indoor hall. To stress the MIMO spatial multiplexing nature, channel power is normalized for each measurement position to retain fixed received SNR. Contrary to the common sense, the results show that considerable capacity is achieved in indoor LOS scenario but more position-sensitive compared to NLOS cases. The influence of the large scale path loss on MIMO capacity is also investigated to reach a comprehensive understanding of indoor MIMO channel characteristics. The measured maximum channel eigenvalue p.d.f. is found to fit t Location-Scale distribution rather than Gamma distribution. Ricean K-factor and spatial correlation are given to provide an intuitive explanation to the observed phenomenon.

The remainder of this paper is organized as follows: Section II describes the measurement system and campaign. Section III introduces the evaluation of wideband MIMO channel capacity. Detailed results are presented in Section IV. In Section V, a summary of this paper is given.

II. Measurement Description

A. Measurement System

Measurement was performed in a teaching building of Beijing University of Posts and Telecommunications utilizing the Elektrobit PropSound Channel Sounder system illustrated in Fig. 1. External RF conversion modules are deployed at both transmit and receive sides to support the operating frequency 6 GHz. Uniform linear array (ULA) with four dipoles has

978-1-4673-5939-9/13/$31.00 ©2013 IEEE

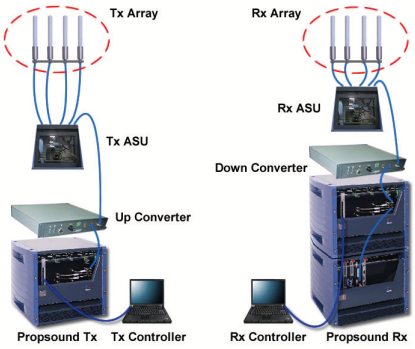

Fig. 1. The setup of the MIMO channel measurement system.

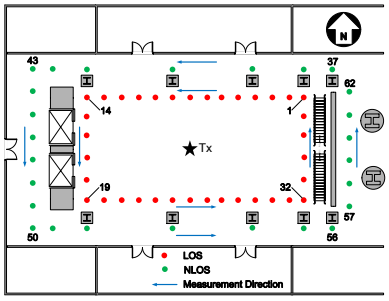

Fig. 2. Measurement layout and measurement position map for LOS and NLOS propagation scenarios.

been equipped at both sides, which can be replaced by omni-directional array (ODA) to extract spatial angle parameters of multipaths. One complete set of MIMO channel realization called cycle is captured in a time-division multiplexing (TDM) method. The measurement of each antenna pairs is accomplished with the help of the high speed antenna switching unit (ASU) to transfer the antennas in sequence. Before the measurement, a back-to-back test is required to obtain the system response for calibration purpose, where the transmitter and receiver are connected directly by cable using a 50 dB attenuator to prevent power overload at the receiver.

B. Measurement Campaign

The measurement was conducted in a typical indoor hall. The layout and measurement position arrangement are shown in Fig. 2, where the measurement position index and moving direction are marked out. The red and green colors represent LOS and NLOS propagations respectively. The height of the Tx array marked by black pentacle is 3m. The Tx array remained stationary in the center of the hall during the experiment. The channel is sampled in a fixed-position method. The receiver moved to the next measurement position once more than 700 sets of channel realizations are collected. The separation between two adjacent LOS measurement positions is 1.6 m (32 wavelengths). Several NLOS measurement positions behind the square columns (1.2m×1.2m), concrete walls and evaluators are deliberately planned for comparison purpose. Total number of LOS and NLOS measurement positions are 36 and 26 respectively. Reflected and scattered components are created by the surrounding walls, columns, evaluators, staris and people. The detailed measurement configuration is listed in Table I.

TABLE I
MEASUREMENT CONFIGURATION

Items	Settings
Center Frequency (GHz)	6
Bandwidth (MHz)	100
PN Code Length (chips)	255
Type of Antenna	ULA
Number of Transmit antenna	4
Number of Receive antenna	4
Element Space of Tx (λ)	1
Element Space of Rx (λ)	0.5
Height of Tx Antenna (m)	3
Height of Rx Antenna (m)	1.8

III. WIDEBAND MIMO CHANNEL CAPACITY

A. Capacity Evaluation

The channel impulse response h_{ij} between the i-th receive and j-th transmit element of a frequency-selective fading MIMO channel $\mathbf{H} \in \mathcal{C}^{N_r \times N_t}$ can be represented as

$$h_{ij}(k) = \sum_{l=0}^{L-1} h_{ij}^{l} \delta(k-l) \tag{1}$$

where L denotes the numbers of effective MPC determined by the measurement bandwidth and the maximum excess delay, and h_{ij}^{l} is the complex fading coefficients of the l-th MPC.

Equal power allocation yields similar performance as water filling in the high SNR region [10], and the relative short access distance in indoor scenario will result in considerable SNR at the receiver. Hence, uniform power allocation scheme among all the antennas is utilized assuming no channel state knowledge available at the transmitter. Supposing $N_t \geq N_r$, the capacity of wideband MIMO channel $\mathbf{H}$ is caculated in a MIMO-OFDM approach as

$$C = \frac{1}{F} \sum_{f=1}^{F} \log_2 \det \left(\mathbf{I} + \frac{P_T}{N_t \sigma_n^2} \mathbf{H}_f \mathbf{H}_f^H \right) \tag{2}$$

where P_T is the total transmit power, and σ_n^2 is the noise power. $\mathbf{H}_f$ is the channel matrix of the f-th subcarrier, and the total number of subcarriers is F which ensures that each subchannel is flat fading. The influence of the path loss is usually removed to highlight the spatial multiplexing nature of the channel. The power normalized channel can be written as

$$\overline{\mathbf{H}}_f = \frac{1}{\sqrt{\eta}} \mathbf{H}_f \tag{3}$$

where η is the environment dependent power normalized factor that denotes the average path gain between the transmit and receive antenna pair, calculated as following [11]

$$\eta = \frac{1}{N_t N_r F} \sum_{f=1}^{F} \sum_{i=1}^{N_r} \sum_{j=1}^{N_t} \left| \mathbf{H}_f^{ij} \right|^2. \tag{4}$$

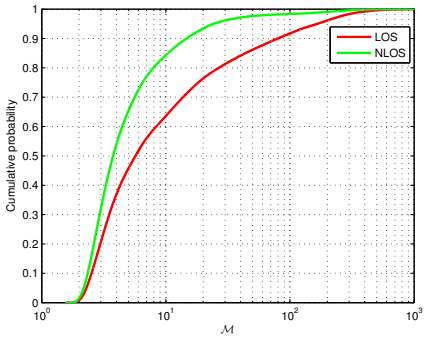

Fig. 3. Multiplexing metric comparison between LOS and NLOS cases.

The capacity of the power normalized channel with fixed received SNR can be calculated as

$$C = \frac{1}{F}\sum_{f=1}^{F}\log_2\det\left(\mathbf{I}+\frac{\rho}{N_t}\overline{\mathbf{H}}_f\overline{\mathbf{H}}_f^H\right) = \frac{1}{F}\sum_{f=1}^{F}\sum_{k=1}^{N_r}\log_2\left(1+\frac{\rho}{N_t}\lambda_k^f\right) \tag{5}$$

where λ_k^f is the k-th eigenvalue of $\overline{\mathbf{H}}_f\overline{\mathbf{H}}_f^H$, and ρ is the received SNR.

$$\rho = \frac{P_T\eta}{\sigma_n^2}. \tag{6}$$

B. Ricean K-factor

The Ricean K-factor is a statistical parameter that reflects the composition of the received signal, defined as the power ratio of the direct and multipath components. The estimation of the Ricean K-factor using a simple moment method [12] is given by

$$K = \frac{\sqrt{G_a^2 - G_v^2}}{G_a - \sqrt{G_a^2 - G_v^2}} \tag{7}$$

where G_a and G_v are the average and root mean square power fluctuation of the received signal respectively.

C. Spatial Correlation

The transmit side correlation value of the l-th MPC between the i-th and j-th transmit antenna is defined as [4]

$$r_{l,ij}^{Tx} = \frac{E\left[h_{mi}^l {h_{mj}^l}^*\right] - E\left[h_{mi}^l\right]E\left[{h_{mj}^l}^*\right]}{\sqrt{\left(E\left[\left|h_{mi}^l\right|^2\right] - \left|E\left[h_{mi}^l\right]\right|^2\right)\left(E\left[\left|h_{mj}^l\right|^2\right] - \left|E\left[h_{mj}^l\right]\right|^2\right)}} \tag{8}$$

and the receive side correlation follows the similar definition.

IV. Measurement Results and Analysis

The systematic channel capacity analysis results are presented in this section. Under the fixed received SNR assumption, the capacity sensitivity to the measurement positions is first investigated in both LOS and NLOS scenarios. Considering the significant received signal power difference between the LOS and NLOS cases, the influence of the path loss on the capacity is then studied. Finally, the channel eigenvalue distribution, Ricean K-factor and spatial correlation analysis results are given. Note the i-th measurement position is denoted as Pos.i in following.

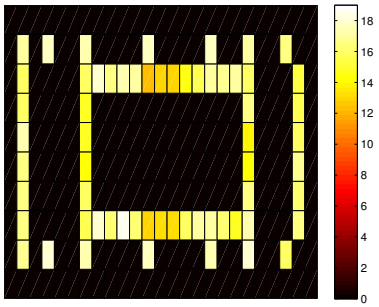

(a) Capacity layout.

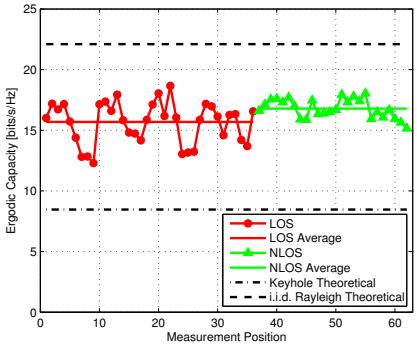

(b) Capacity vs. measurement position.

Fig. 4. Ergodic capacity with fixed received SNR (20 dB).

A. Channel Condition

We first use the multiplexing metric proposed in [13] to compare the channel conditions between indoor LOS and NLOS scenarios, defined as

$$\mathcal{M} = \frac{\|\mathbf{H}\|_F^2}{\|\mathbf{H}\|_F^2 - \lambda_{\max}} \tag{9}$$

The CDF comparison of the multiplexing metric between LOS and NLOS scenarios is given in Fig. 3. The probability $\Pr(\mathcal{M} \le 10)$ is about 64% and 85% in LOS and NLOS respectively, which indicates that considerable channel capacity can be achieved in indoor LOS scenario. In following, we present the detailed capacity analysis results to verify it.

B. Capacity with Fixed Received SNR

To highlight the spatial multiplexing essence of the MIMO channel, power normalized operation is processed first for each measurement position to remove the influence of large scale path loss and shadow fading. The ergodic capacity results are given in Fig. 4, and the capacity layout corresponding to the measurement position map is also plotted. The average capacity in LOS cases is 15.69 bit/s/Hz and only about

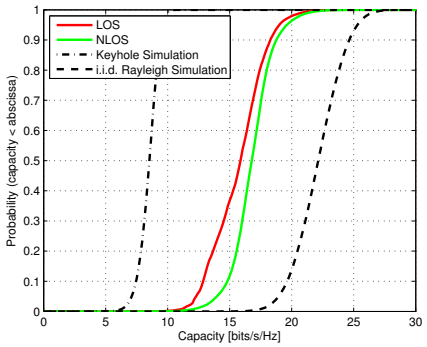

Fig. 5. Outage capacity comparison between LOS and NLOS cases at 20 dB.

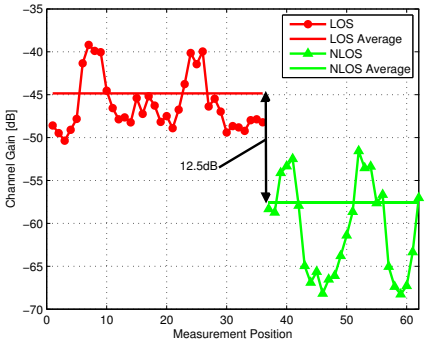

Fig. 6. Average channel gain vs. measurement position.

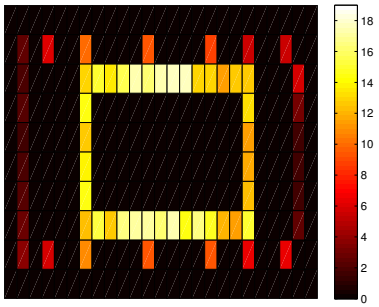

(a) Capacity layout.

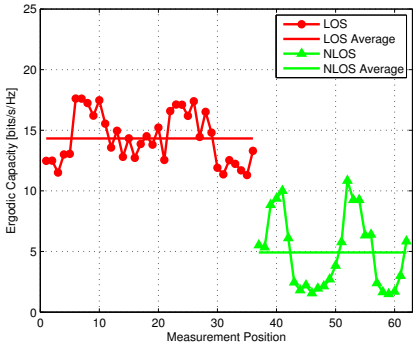

(b) Capacity vs. measurement position.

Fig. 7. Ergodic capacity with fixed transmit power, and the average LOS SNR is 20 dB.

1.1 bit/s/Hz less than that in NLOS cases. The theoretical capacity value of the keyhole and narrowband i.i.d. Rayleigh fading MIMO channel are also plotted as the lower and upper bound respectively for reference. Contrary to the common knowledge, it indicates that considerable capacity is achieved in indoor LOS scenario. However, the capacity fluctuation level in Fig. 4(b) reveals that the capacity in LOS cases is more position-sensitive than that in NLOS cases. The channel capacity sensitivity to the antenna array displacement and orientation is also studied in [14] for optimized LOS MIMO system in indoor environment. Low capacity occurs in the LOS positions Pos.7-Pos.9 and Pos.24-Pos.26.

Outage capacity comparison between the LOS and NLOS scenarios is also given in Fig. 5 . It can be seen that the outage capacity gap between the LOS and NLOS cases is a little larger than the average ergodic capacity gap (e.g. the 10% outage capacity in LOS cases is about 2.2 bits/s/Hz lower than that in NLOS cases). The reason is the existence of "bad positions" (e.g. Pos.7-Pos.9 and Pos.24-Pos.26, see Fig. 4(b)) which yield significant lower capacity.

C. Capacity with Fixed Transmit Power

In reality, the received signal will suffer different path loss as the movements of the receiver, which will result in fluctuant received SNR for fixed transmit power. The path loss difference between the LOS and NLOS scenarios should be taken into account for a practical fair performance evaluation. The average channel gain of each measurement position is given in Fig. 6 in both LOS and NLOS cases. The transmit power is adjusted to an appropriate level that ensure the average received SNR in LOS cases is 20dB which is about 12.5dB higher than that in NLOS cases.

It is clear that the spatial distribution of the capacity in Fig. 7(a) shows a shadow-like layout. Contrary to the results with fixed received SNR metric, the average ergodic capacity in NLOS cases is only 4.92bits/s/Hz which is evidently lower than the LOS cases. The reason is that the absence of direct path will cause a remarkable received SNR drop in NLOS scenario. The positions behind the square column (Pos.39-Pos.41 and Pos.52-Pos.54) suffer relatively slight capacity degradation. Note that the "bad positions" are no more the worst cases (see Fig. 4(b)) due to the significant SNR boost (closest to the transmitter) indicated in Fig. 6.

D. Channel Eigenvalue Distribution

The maximum channel eigenvalue is a key parameter to assess the SER and outage probability of the MIMO beamforming systems. Also the minimum eigenvalue is important for adaptive MIMO system switching between diversity and multiplexing schemes [15]. The MIMO channel eigenvalue p.d.f. in outdoor NLOS environment is found to match Gamma distribution [9]. But the channel will yield rather different

characteristic in indoor scenario due to the dominated LOS propagation, low-speed scatters and the closed building structure. The measured eigenvalue p.d.f. and distribution fitting in both LOS and NLOS cases are plotted in Fig. 8 and Fig. 9. The measured maximum eigenvalue p.d.f. presents narrow sharp peak mainly due to the relative static channel (e.g. stationary scatters and slow moving people) in indoor scenario. It is clear that t Location-Scale distribution can provide much better fitting than Gamma distribution. The p.d.f. of the t Location-Scale distribution [16] is

$$f(x) = \frac{\Gamma\left(\frac{\nu+1}{2}\right)}{\sigma\sqrt{\pi\nu}\Gamma\left(\frac{\nu}{2}\right)}\left[1+\frac{1}{\nu}\left(\frac{x-\mu}{\sigma}\right)^2\right]^{-\left(\frac{\nu+1}{2}\right)} \quad (10)$$

where μ is the location parameter, while $\sigma > 0$ and $\nu > 0$ are the scale and shape parameter respectively. If x has a t Location-Scale distribution, then $\frac{x-\mu}{\sigma}$ will satisfy Student's t distribution with ν degrees of freedom. Moreover, it approaches Normal distribution when ν takes an infinity value. It must be pointed out that other distributions are also compared but don't give corresponding results owing to their bad fitting. However, the Gamma distribution seems to be a good fitting for the measured minimum eigenvalue.

E. Ricean K-factor and Spatial Correlation

Generally, the channel capacity is greatly influenced by the richness of the multipaths and the spatial correlation of the dominated MPCs. As indicated in Fig. 10, the fluctuation level of the Ricean K-factor in LOS scenario is more obvious than that in NLOS scenario, which is coherently related to the position-sensitive characteristic of the indoor LOS channel capacity. In following, we present the averaged power delay profile and spatial correlation results for typical LOS and NLOS measurement positions to provide an explanation to the observed phenomenon. The Pos.9 and Pos.22 yield the lowest and highest capacity in LOS scenario (see Fig. 4), and the Pos.51 is a typical NLOS measurement position. The corresponding averaged power delay profiles and spatial correlations are given in Fig. 11 and Fig. 12. The joint effect of the MPC richness and the spatial correlation will lead to the signficant capacity fluctuation (position-sensitive) in indoor LOS scenario. The CDF comparison of the multiplexing metric is also given in Fig. 13. The mentioned "bad positions" all yield high K-factor and spatial correlation values, and consequently leading to low channel capacity.

The position-sensitive phenomenon of the channel capacity suggests that it is possible to enhance the average spectrum efficiency through appropriate geometry-based approach in some indoor LOS scenarios. Taking an indoor conference room for example, most of the data traffic is generated by the user equipments surrounding the conference table (hottest spot). It is worthwhile in practice to enhance the average data throughput focusing on the user equipments within the hottest spot. The mentioned geometry-based approach involves the optimization of the access point (AP) position, antenna element spacing and the orientation of the antenna array at the AP side.

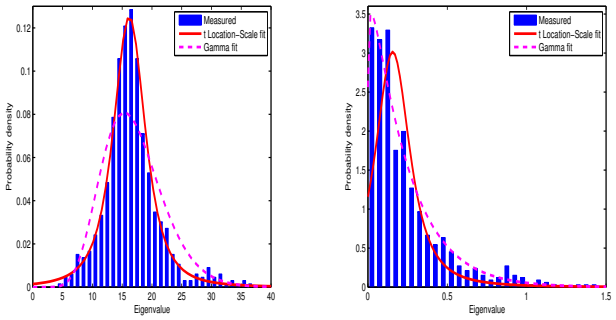

(a) Maximum eigenvalue. (b) Minimum eigenvalue.

Fig. 8. The measured eigenvalue p.d.f. and t Location-Scale, Gamma fitting in typical LOS case.

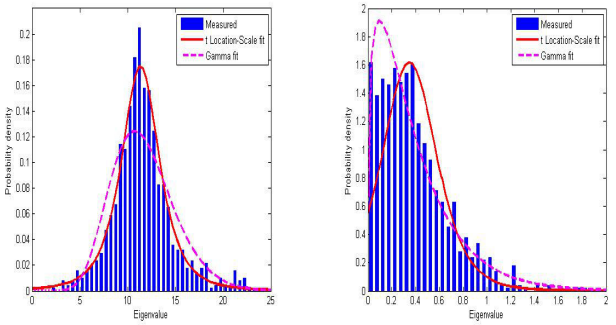

(a) Maximum eigenvalue. (b) Minimum eigenvalue.

Fig. 9. The measured eigenvalue p.d.f. and t Location-Scale, Gamma fitting in typical NLOS case.

V. Conclusion

In this paper, wideband MIMO channel capacity comparison between the LOS and NLOS scenarios is presented based on the channel measurement in a typical indoor environment at 6 GHz. For the fixed received SNR, considerable capacity is achieved in LOS cases but more position-sensitive than that in NLOS cases. The observed phenomenon indicates that it is possible to enhance the average spectrum efficiency in some typical indoor LOS scenarios by certain geometry-based optimization method. Low capacity is observed when the receiver is close to the transmitter in LOS scenario, which yield high K-factor and spatial correlation values. When taking the large scale path loss influence into account, the capacity in LOS cases greatly outperforms that in NLOS cases. The measured maximum channel eigenvalue p.d.f. is found to fit t Location-Scale distribution in indoor scenarios.

Acknowledgment

The research is supported in part by China Important National Science & Technology Specific Projects under Grant NO.2012ZX03001043-009 and NO.2012ZX03006003-003, and by Program for New Century Excellent Talents in University of Ministry of Education of China NCET-11-

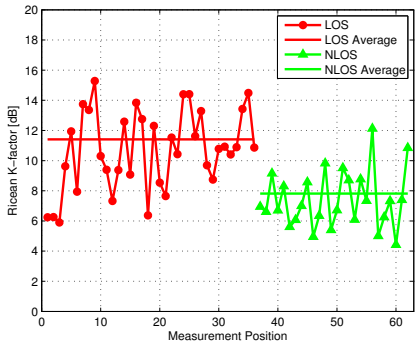

Fig. 10. Ricean K-factor vs. measurement position

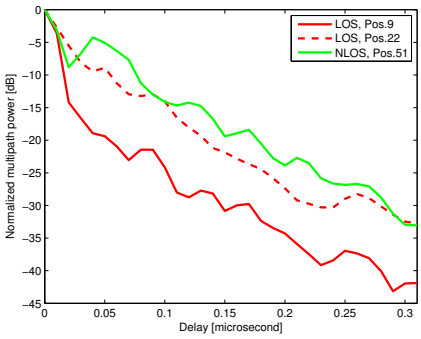

Fig. 11. Averaged power delay profile for typical LOS and NLOS measurement positions.

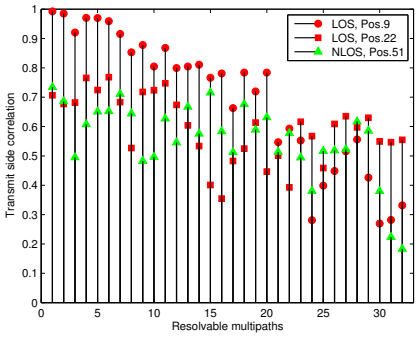

Fig. 12. Transmit side spatial correlation ($r_{l,14}^{Tx}$) of resolvable multipaths for typical LOS and NLOS measurement positions.

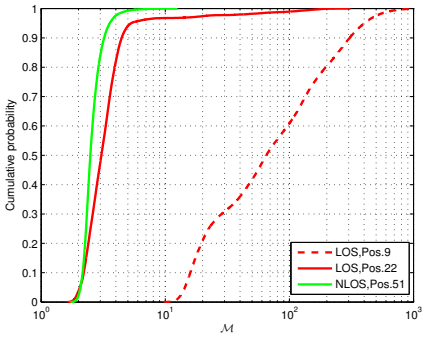

Fig. 13. Multiplexing metric CDF comparisons between different LOS and NLOS measurement positions.

0598, also by Telecommunications Science Technical Institute (Datang Telecommunication Technology and Industry Group).

REFERENCES

[1] A. Ghosh, R. Ratasuk, B. Mondal, N. Mangalvedhe, and T. Thomas, "LTE-Advanced: next-generation wireless broadband technology [invited paper]," *IEEE Wireless Commun.*, vol. 17, no. 3, pp. 10 –22, Jun. 2010.

[2] X. Gao, J. Zhang, and Y. Zhang, "Eigenvalue statistics and spatial characteristics in hotspot areas based on wideband MIMO channel measurements," in *Proc. IEEE Vehicular Technology Conf.*, Sept. 2008, pp. 1 –5.

[3] J. Gupta, H. Suzuki, and K. Ziri-Castro, "Effect of pedestrian movement on MIMO-OFDM channel capacity in an indoor environment," *IEEE Antennas and Wireless Propagation Letters*, vol. 8, pp. 682 –685, 2009.

[4] P. Kafle, A. Intarapanich, A. Sesay, J. McRory, and R. Davies, "Spatial correlation and capacity measurements for wideband MIMO channels in indoor office environment," *IEEE Trans. on Wireless Commun.*, vol. 7, no. 5, pp. 1560 –1571, May 2008.

[5] J. Poutanen, J. Salmi, K. Haneda, V. Kolmonen, and P. Vainikainen, "Angular and shadowing characteristics of dense multipath components in indoor radio channels," *IEEE Trans. on Antennas and Propagation*, vol. 59, no. 1, pp. 245 –253, Jan. 2011.

[6] X. NIE, J. ZHANG, and P. ZHANG, "Polarization and spatial statistic of wideband MIMO relay channels in urban environment at 2.35 GHz," *IEICE TRANS. COMMUN.*, vol. E94-B, no. 1, pp. 139 –149, Jan. 2011.

[7] D. Dong, J. Zhang, Y. Zhang, and X. Nie, "Large scale characteristics and capacity evaluation of outdoor relay channels at 2.35 GHz," in *Proc. IEEE Vehicular Technology Conf.*, Sept. 2009, pp. 1 –5.

[8] S. Jin, M. McKay, X. Gao, and I. Collings, "MIMO multichannel beamforming: SER and outage using new eigenvalue distributions of complex noncentral wishart matrices," *IEEE Trans. on Commun.*, vol. 56, no. 3, pp. 424–434, Mar. 2008.

[9] W. Kim, H. Lee, J. J. Park, M.-D. Kim, and H. K. Chung, "Distribution of eigenvalues for 2×N MIMO channel capacity based on urban microcell measurements," in *IEEE Int. Symposium on Personal Indoor and Mobile Radio Commun.*, Sept. 2010, pp. 223 –228.

[10] S. Ye and R. Blum, "Optimized signaling for mimo interference systems with feedback," *IEEE Trans. on Signal Processing*, vol. 51, no. 11, pp. 2839 – 2848, Nov 2003.

[11] V. Jungnickel, S. Jaeckel, L. Thiele, L. Jiang, U. Kruger, A. Brylka, and C. von Helmolt, "Capacity measurements in a cooperative MIMO network," *IEEE Trans. on Vehicular Technology*, vol. 58, no. 5, pp. 2392 –2405, Jun 2009.

[12] L. Greenstein, D. Michelson, and V. Erceg, "Moment-method estimation of the Ricean K-factor," *IEEE Commun. Letters*, vol. 3, no. 6, pp. 175 –176, Jun 1999.

[13] J. Gao, J. Zhang, Y. Xiong, Y. Sun, and X. Tao, "Performance evaluation of closed-loop spatial multiplexing codebook based on indoor MIMO channel measurement," *International Journal of Antennas and Propagation*, vol. 2012, 2012.

[14] I. Sarris and A. Nix, "Design and performance assessment of high-capacity MIMO architectures in the presence of a line-of-sight component," *IEEE Tran. on Vehicular Technology*, vol. 56, no. 4, pp. 2194–2202, Jul. 2007.

[15] R. Heath and A. Paulraj, "Switching between diversity and multiplexing in MIMO systems," *IEEE Trans. on Commun.*, vol. 53, no. 6, pp. 962–968, Jun. 2005.

[16] MathWorks. t Location-Scale distribution. [Online]. Available: http://www.mathworks.cn/help/toolbox/stats/brn2ivz-145.html